

# Formation of Oxide Nano-Particles in Flames

C. Janzen, H. Orthner and P. Roth

Institut für Verbrennung und Gasdynamik  
Gerhard-Mercator-Universität Duisburg  
47048 Duisburg, Germany  
roth@ivg.uni-duisburg.de

## Abstract

A low pressure flat premixed  $H_2/O_2/Ar$  flame doped with different precursors was used to produce nanosized silica, alumina, and tin-oxide particles. The gaseous and liquid precursors silane ( $SiH_4$ ), trimethylaluminum ( $Al(CH_3)_3$ ), and tetramethyltin ( $Sn(CH_3)_4$ ), respectively, were used as source materials in different concentrations. The particles were characterized due to their composition, specific surface area, morphology, and size utilizing FT-IR spectroscopy, BET analysis by nitrogen absorption, X-ray diffraction, transmission electron microscopy, and particle mass spectrometry. It has been shown that the precursor concentration along with flame temperature are the most important factors for particle size, shape, and structure. In the case of  $SnO_2$  formation, two distinct lattice structures could be identified depending on the exposure time in the hot flame gases during sampling.

## Introduction

The formation of oxide particles in flames is widely used for the production of e.g. ceramics, semiconductors, or fiber optics. The comparably simple setup and the easy scale-up of these processes allow the production of large quantities of powders having certain characteristics. Several types of flame reactors have been in the focus of many researchers in the past, including diffusion, counter-flow diffusion, and premixed flames, see for example [1, 2, 3]. In the present work, the formation of tin-oxide ( $SnO_2$ ), silica ( $SiO_2$ ), and alumina ( $Al_2O_3$ ) is studied in a laminar premixed low pressure  $H_2/O_2/Ar$  flame doped with respective precursors. The characteristics of the flame generated particles were studied applying infrared spectroscopy, X-ray diffraction, TEM analysis, and *in-situ* particle mass spectrometry, PMS [3].

## Experimental

The experimental setup used in this study consists of the low pressure flame reactor and two thermophoretic sampling devices. A detailed description is given in [3]. Different amounts of the metalorganic precursors silane, tetramethyltin (TMT,  $Sn(CH_3)_4$ ), and trimethylaluminum (TMA,  $Al(CH_3)_3$ ), respectively, were added to the burner stabilized flame. The hydrogen-oxygen flame was burnt under lean condition with a  $H_2/O_2$  ratio of 1.69. Argon was added as diluent in order to vary the flame temperature. The molar ratio, with respect to the reactive gases was 1.36. The metalorganic precursors were vaporized and mixed with Ar by the partial pressure method in a mixing vessel. The two aerosol sample devices consist of a cooled substrate disposed inside the reaction chamber and an electrically driven chain transmission for the deposition of particle samples on commercial TEM grids. For the *in-situ* particle mass spectrometry, molecular beam samples were taken from the flame gases and analysed due to particle mass [3].

## Results and Discussion

In a series of experiments the properties of flame generated oxide nano-particles were investigated by the above mentioned *ex-situ* methods. The dependence of BET surface area, composition, and size from the amount of dopant in the flame was studied by variation of the precursor gas flow. FT-IR measurements in general show that the solid phase formed in the low-pressure flames are the expected oxidation product of the respective metal in the flame.

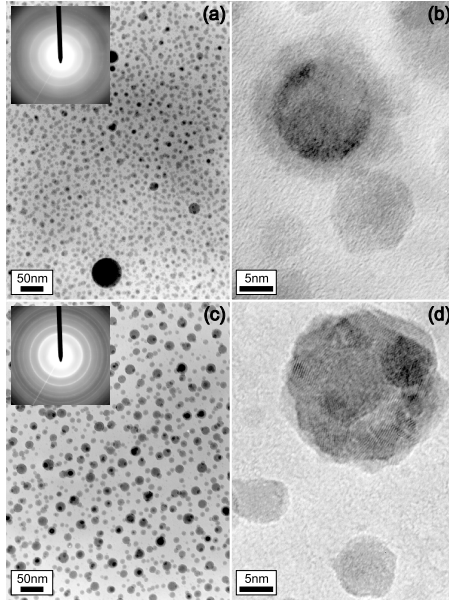


Figure 1: TEM micrographs of  $\text{SnO}_2$  particles deposited directly on TEM grids. Precursor hang concentration: 663 ppm. Sample position:  $x = 25 \text{ mm}$  (a,b),  $x = 60 \text{ mm}$  (c,d).

Samples of  $\text{SnO}_2$  particles on TEM grids reveal (see Fig. 1) that the particles are a mixture of orthorhombic  $\text{SnO}$  and the high-temperature  $\beta$ -phase of  $\text{SnO}_2$ . The  $\text{SnO}_2$  samples for the TEM micrographs were extracted from a flame burning 663 ppm  $\text{Sn}(\text{CH}_3)_4$ , the sample position was  $x = 25 \text{ mm}$  and  $x = 60 \text{ mm}$ , respectively. The particles of Fig. 1 (a), (b) exhibit a relatively wide spread distribution ranging from 5 nm to 20 nm. Electron diffraction pattern show a low degree of crystallinity of these particles. From the magnified extract shown in part (b), it can be deduced that the initial flame reaction product,  $\text{SnO}$ , oxidizes from the outer shell to the inner core to form  $\text{SnO}_2$  [4]. In contrast, particles sampled at  $x = 60 \text{ mm}$ , see Fig. 1 part (c) and (d), are larger and more crystalline due to the longer exposure time in the hot flame gases though they exhibit the same crystal structure as found at early stages in the flame. Primary particles of  $d_P = 8.3 \text{ nm}$  as well as spherical agglomerates of about  $d_{agg} = 22 \text{ nm}$  form the main fraction of the particle sample. The agglomerates exhibit a certain porosity indicating incomplete coalescence.

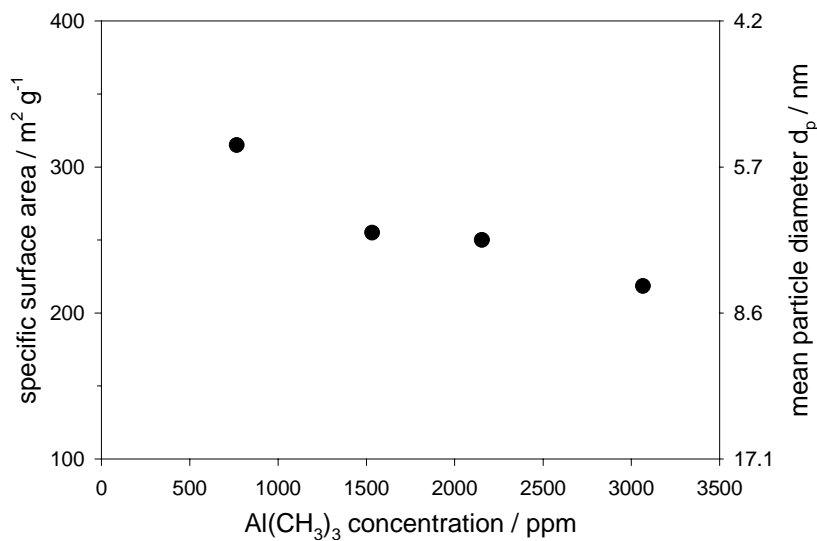


Figure 2: Specific surface area of flame generated alumina particles.  $d_P = 6000/(\rho_P \cdot \text{BET})$ . hang Flame conditions:  $\text{H}_2/\text{O}_2 = 1.69$ ,  $\text{Ar}/(\text{H}_2 + \text{O}_2) = 1.36$ ,  $v_u = 1.32 \text{ m s}^{-1}$ ,  $p_B = 30 \text{ mbar}$ .

The influence of the initial  $\text{Al}(\text{CH}_3)_3$  precursor concentration on the mean particle size was inves-

tigated by determining the BET surface of collected powders. The results are shown in Fig. 2. The sample were taken at  $x = 60 \text{ mm}$  above the burner head, the detailed burning conditions are given in the figure caption. It is obvious that the specific surface area decreases from  $315 \text{ m}^2 \text{ g}^{-1}$  to  $220 \text{ m}^2 \text{ g}^{-1}$  with increasing initial  $\text{Al}(\text{CH}_3)_3$  concentration indicating the growth of the mean particle diameter from  $5.4 \text{ nm}$  to  $7.8 \text{ nm}$ .

The evolution of the mean particle size with the flow coordinate of silica particles generated in silane doped flames is summarized in Fig. 3. Here, the mean particle mass and the respective diameter are plotted against precursor concentration for three distances from the burner head. It is obvious that the measured mean particle mass increases with increasing initial concentration of the dopant. The dependence on the distance from the burner head is not very distinct in the range  $20 \text{ mm} \leq x \leq 40 \text{ mm}$ .

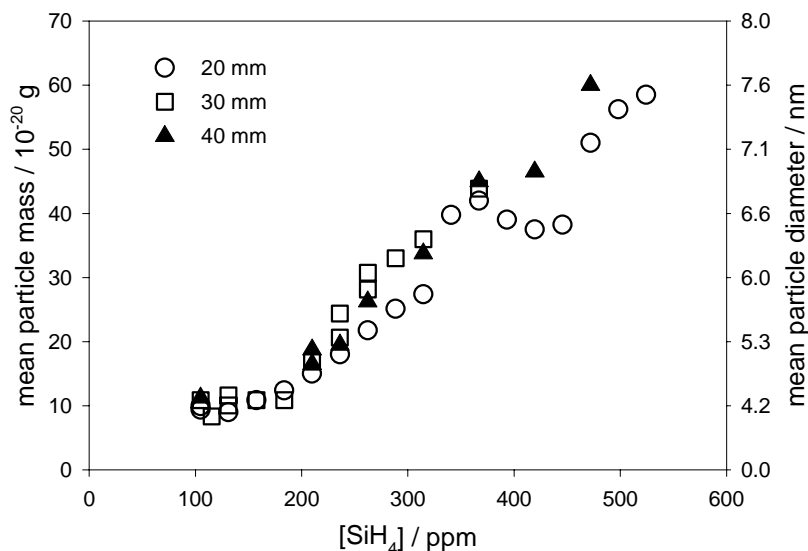


Figure 3: Particle size measurements of  $\text{SiO}_2$ -particles as a function of precursor concentration. hang Flame conditions:  $\text{H}_2/\text{O}_2 = 1.69$ ,  $\text{Ar}/(\text{H}_2 + \text{O}_2) = 1.36$ ,  $v_u = 1.32 \text{ m s}^{-1}$ ,  $p_B = 30 \text{ mbar}$ .

## Acknowledgment

The financial support of the German National Science Foundation (DFG) is gratefully acknowledged.

## References

- [1] C.-H. Hung and J. L. Katz.  
Formation of mixed oxide powders in flames: Part I.  
 $\text{TiO}_2\text{-SiO}_2$ .  
*J. Mater. Res.*, 7:1861–1869, 1992.
- [2] G.D. Ulrich.  
Theory of Particle Formation and Growth in Oxide Synthesis Flames.  
*Combust. Sci. and Tech.*, 4:47–57, 1971.
- [3] D. Lindackers, M.G.D. Strecker, P. Roth, C. Janzen, and S.E. Pratsinis.  
Formation and growth of  $\text{SiO}_2$  particles in low pressure  
 $\text{H}_2/\text{O}_2/\text{Ar}$  flames doped with  $\text{SiH}_4$ .  
*Combust. Sci. and Tech.*, 123:287–315, 1997.
- [4] B. Rellinghaus, D. Lindackers, M. Köckerling, P. Roth, and E.F. Wassermann.  
Structural properties of flame generated  $\text{SnO}_2$  nano-particles.  
*submitted to Eur. Phys. J. B*, 1998.